Coded excitation speeds up the detection of the fundamental flexural guided wave in coated tubes

Xiaojun Song, Petro Moilanen, Zuomin Zhao, Dean Ta, Jalmari Pirhonen, Ari Salmi, Edward Hæeggström, Risto Myllylä, Jussi Timonen, and Weiqi Wang

---

Articles you may be interested in

Tailoring the excitation of fundamental flexural guide waves in coated bone by phase-delayed array: Two-dimensional simulations
J. Acoust. Soc. Am. **137**, 1134 (2015); 10.1121/1.4908312

DETECTION OF AXIAL CRACKS IN TUBE AND PIPE USING TORSIONAL GUIDED WAVES
AIP Conf. Proc. **975**, 193 (2008); 10.1063/1.2902658

Flexural Torsional Guided Wave Pipe Inspection
AIP Conf. Proc. **820**, 181 (2006); 10.1063/1.2184527

Circumferential Guided Waves for Defect Detection in Coated Pipe
AIP Conf. Proc. **820**, 165 (2006); 10.1063/1.2184525

The speed of a tube wave
J. Acoust. Soc. Am. **87**, 414 (1990); 10.1121/1.399262

Coded excitation speeds up the detection of the fundamental flexural guided wave in coated tubes

Xiaojun Song,[1,a] Petro Moilanen,[2,a] Zuomin Zhao,[3] Dean Ta,[4,5,b]
Jalmari Pirhonen,[2] Ari Salmi,[6] Edward Hæeggström,[6] Risto Myllylä,[3]
Jussi Timonen,[2] and Weiqi Wang[4]

[1]*Department of Electronic Science and Technology, Shanghai University of Electric Power, Shanghai 200090, China*
[2]*Department of Physics, University of Jyväskylä, Jyväskylä, Finland*
[3]*Department of Electrical Engineering, University of Oulu, Oulu, Finland*
[4]*Department of Electronic Engineering, Fudan University, Shanghai 200433, China*
[5]*Key Lab of Med Imag Computing and Computer-Assisted Intervention (MICCAI), Shanghai, 200032 China*
[6]*Department of Physics, University of Helsinki, Helsinki, Finland*

The fundamental flexural guided wave (FFGW) permits ultrasonic assessment of the wall thickness of solid waveguides, such as tubes or, e.g., long cortical bones. Recently, an optical non-contact method was proposed for ultrasound excitation and detection with the aim of facilitating the FFGW reception by suppressing the interfering modes from the soft coating. This technique suffers from low SNR and requires iterative physical scanning across the source-receiver distance for 2D-FFT analysis. This means that SNR improvement achieved by temporal averaging becomes time-consuming (several minutes) which reduces the applicability of the technique, especially in time-critical applications such as clinical quantitative ultrasound. To achieve sufficient SNR faster, an ultrasonic excitation by a base-sequence-modulated Golay code (BSGC, 64-bit code pair) on coated tube samples (1-5 mm wall thickness and 5 mm soft coating layer) was used. This approach improved SNR by 21 dB and speeded up the measurement by a factor of 100 compared to using a classical pulse excitation with temporal averaging. The measurement now took seconds instead of minutes, while the ability to determine the wall thickness of the phantoms was maintained. The technique thus allows rapid noncontacting assessment of the wall thickness in coated solid tubes, such as the human bone. © *2016 Author(s). All article content, except where otherwise noted, is licensed under a Creative Commons Attribution (CC BY) license (http://creativecommons.org/licenses/by/4.0/).* [http://dx.doi.org/10.1063/1.4962400]

I. INTRODUCTION

Guided waves (GW) are widely used for non-destructive testing.[1] These mechanical stress waves propagate along elongated structures and are sensitive to the structural and elastic properties of the inspected bodies.[2] Due to little loss of energy in long distance propagation, GWs have been widely used in the evaluation of metallic pipelines and other engineering structures.[3,4] Nowadays, GWs are also used for assessment of cortical bone due to its pipe-like structure.[5]

A method that employs a fundamental flexural guided wave (FFGW), consistent with the fundamental antisymmetric Lamb mode (A0), which corresponds to the case of the "free plate", permits an inference of the wall thickness of tubes, e.g. the cortical thickness.[6] However, such

---

[a]These authors made equal contribution.
[b]Corresponding author: Tel.: +86-21-55664473 Fax: +86-21-55664473 E-mail: tda@fudan.edu.cn; tadean.fudan@gmail.com

6, 095001-1

tubular structures are often coated,[7–10] and determining the structural properties of the hard tube wall (or a plate) under a soft coating is challenging due to interference from the wave modes propagating on the coating, which reduces the signal-to-interference ratio (SIR, ratio of the power of the desired mode compared to all other modes). Solutions to increase the SIR include photo-acoustic emission of ultrasound (US)[11] and phase-delayed excitation of US,[12,13] however the signals measured from top of the coating still feature low signal-to-noise ratio (SNR, ratio of the power of the desired mode compared to the noise level). One could also use temporal averaging, but this rapidly increases the measurement duration, which is not suitable for time-critical systems such as samples that are moving, change as a function of time or measurement of living samples *in vivo*.

Coded excitation[14–16] has shown potential for SNR improvement for uncoated tubes[17] using a technique called base-sequence modulated Golay-code (BSGC).[18] This code permits reconstruction of pulse waveforms by effectively reducing the range of the side lobes.[17] A base-sequence modulation reduces the frequency band of the code, which makes the coded waveform less sensitive to dispersion (guided waves) and distortion (US transducers) than the classical Golay codes.[17,19] Despite showing an SNR improvement, our previous study did not focus on two important aspects: measurement duration and possible coating of the samples.

Therefore, the present study aims to show that a BSGC-coded emission speeds up the FFGW measurement of coated tubes with a scanning ultrasound setup, while maintaining the quality of wall-thickness estimation. This study is carried out in coated axisymmetric tubes (that represent human *radius* embraced by soft tissue).

II. MATERIALS AND METHODS

A. Base-sequence-modulated Golay Code

The BSGC was used as described in Ref. 19. Briefly, we used a 16-bit Golay code with $A = [-1, -1, 1, -1, -1, -1, -1, 1, -1, 1, 1, 1, -1, 1, -1, -1]$ and $B = [-1, -1, 1, -1, -1, -1, -1, 1, 1, -1, -1, -1, 1, -1, 1, 1]$ and a 4-bit base sequence $S = [1, 1, 1, 1]$. Each bit in S was expressed by one period of a sine wave. S was also used as the classical (*i.e.*, uncoded) pulse waveform, Fig. 1(a) (blue). Figure 2(a) (green and cyan) shows A and B, featuring a code length of $N = 4 \cdot 16 = 64$ bits.

Decoding the sequences A and B reconstructs S. Golay coding should increase the SNR of the decoded response by a gain factor of[19]

$$SNR_{gain} = SNR_{code} - SNR_{pulse} = 10 \log 2N, \tag{1}$$

where N is the number of bits in the code. Thus, prolonging the emission sequence improves SNR, which reduces the need for averaging.

B. Experimental Set-up

Our axial-transmission setup consisted of a conventional contact ultrasound source and an optical receiver (Fig. 1(b)). Both transducers faced the same side of the tube, perpendicular to its surface. The source-receiver distance was adjustable. The transmitter (Ø = 10mm) was a custom-made piezo transducer with a 220 kHz center frequency and 300 kHz (−16dB) bandwidth. We selected this custom-made transducer, since it is related to commercial bone ultrasonometers which operate within a 0.1-1.25 MHz range.[20] An arbitrary waveform generator (Model 5411, National Instruments) generated the driving waveforms for the classical and BSGC excitations. According to theoretical predictions, the excitability of A0 Lamb mode is increased asymptotically towards low ultrasonic frequencies.[21] It is thus predicted that the efficiency of FFGW excitation is significantly enhanced by choosing as low an excitation frequency as possible, here, using a 25, 27, or 30 kHz center frequency, which nearly reaches the low limit of ultrasound. Using such low driving frequencies maximized the SIR of the FFGW[11,13] but reduced SNR by 20-25 dB compared to operating at the center frequency of the piezo transducer's. The classical driving waveforms featured a 48% (−6 dB) fractional bandwidth whereas the BSGC driving waveforms featured 30% (−6 dB) fractional bandwidths, relative to their center frequency. For example, when the excitation
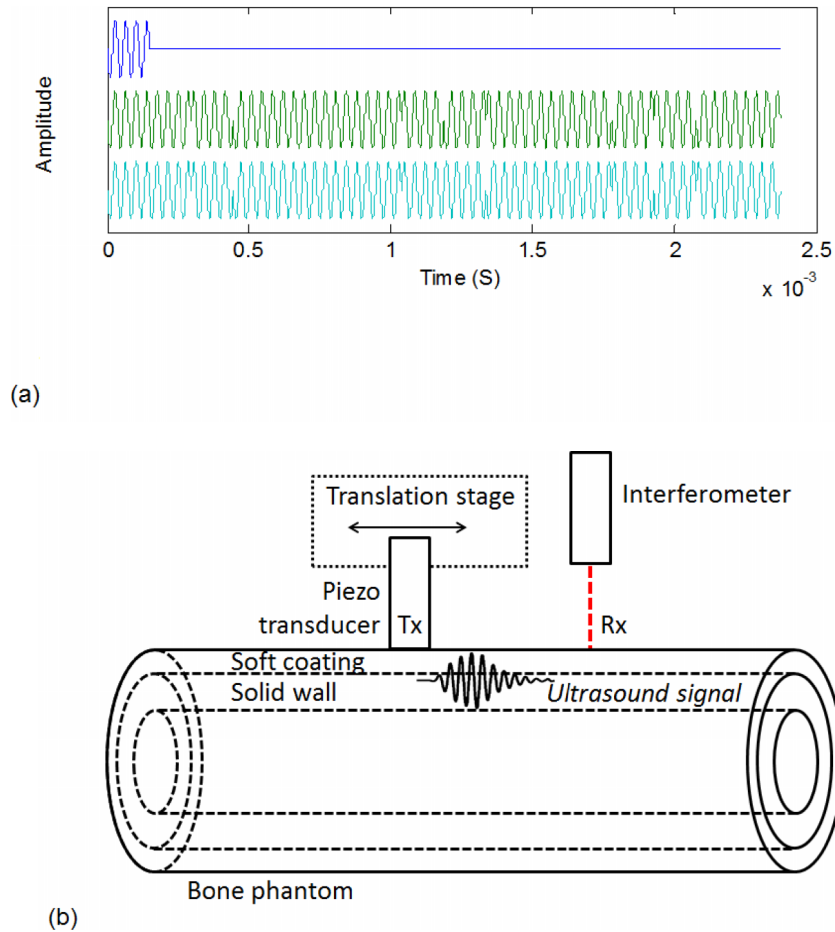
FIG. 1. (a) Excitation waveforms: a classical tone burst (blue), BSGC waveform *A* (green) and BSGC waveform *B* (cyan). (b) Experimental setup.

frequency was 27 kHz, the bandwidth of classical driving waveform would be 13 kHz (−6 dB), and the bandwidth of BSGC driving waveforms was relatively smaller, which would be 8 kHz (−6 dB). The generator provided a 10 V drive amplitude (we refer to this as the 'unamplified excitation'). Additionally, a custom-made amplifier (18 dB; an inverting circuit based on an operational amplifier 3584 by Texas Instruments), provided an excitation amplitude of 80 V. Typically the measurement was made at 40 transmitter to receiver distances, ranging from 20 to 50 mm, corresponding to step size of 0.75 mm.

Signals were received by a custom-made heterodyne interferometer (HeNe, 632.8 nm) with a sub-nanometer displacement resolution and a bandwidth for DC of 8 MHz. The receiving laser probed a fixed position on the sample surface. The carrier frequency of the interferometer was reduced by electrical frequency mixing down to 1 MHz, to permit recording low-frequency (<250 kHz) ultrasound at a 10-MHz sampling frequency (PCI-5124 digitizer, National Instruments). Averaging factors from 4 to 128 were evaluated.

C. Signal Analysis

The received spatio-temporal signals were analyzed by using Matlab (The MathWorks Inc.). A two-dimensional fast Fourier transform (2D-FFT)[22,23] was used to determine the experimental phase velocity of FFGW. To enhance the extraction of FFGW, the received signals were preprocessed by group-velocity filtering according to Ref. 23. The filter parameters were 1600 m.s^{-1} (slope) and 120 μs (the time expansion of the gate window). The start point of the gate window
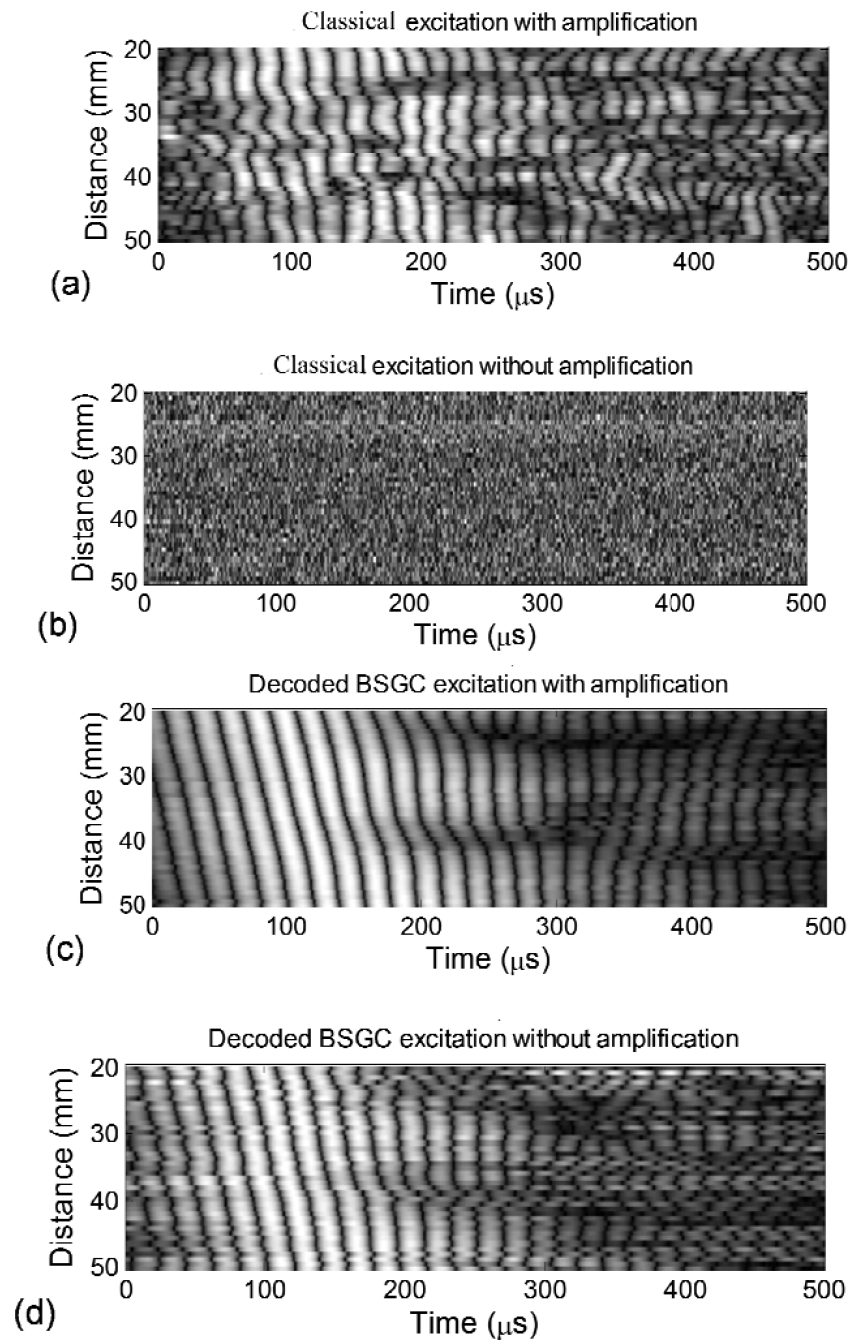
FIG. 2. Measured distance-time diagrams excited by a classical tone burst (a) with an 18-dB amplification (80 V) and (b) without amplification (10 V). Similar diagrams excited by BSGC waveforms (c) with an 18-dB amplification (80 V) and (d) without amplification (10 V). Results are shown for a 25 kHz excitation in a 3-mm tube with a 5-mm coating.

was selected at the first non-zero value of the received signals. Moreover, the classical excitation required noise reduction by a 2D rectangular moving average filter (2.25 mm x 2.0 μs) and a low-pass filter (f_{LP} = 50 kHz; a Hamming-window-based finite-impulse-response filter based on Matlab functions *fir1* and *filter*).

SNR was determined by analyzing temporal waveforms received at 40 transmitter to receiver distances, ranging from 20 to 50 mm. Signal was extracted from noise using a second-order Savitzky-Golay filter with a 5 μs (amplified signal) or 20 μs (unamplified signal) window. The

RMS power of the FFGW signal was determined within a 300 μs window, centered at the peak amplitude of the FFGW wave packet. The RMS power of noise was determined from the unfiltered signal, within a 500 μs window, subsequent to the wave packet, 150 μs apart from the signal window. Reproducibility of the SNR measurement as a function of the source-receiver distance was evaluated by three repeated measurements.

D. Samples

Five axisymmetric tubes (diameter 16 mm; wall thickness 1-5 mm) with a soft coating (5 mm) were used.[11] Solid tubes were custom made from aluminum oxide powder (70% by mass) and epoxy resin. Soft coating was a 1:1 mixture of silicone elastomer and glycerol. The tubes had a bulk compression velocity of $c_L = 3000$ m.s^{-1}, a bulk shear velocity of $c_T = 1550$ m.s^{-1}, and a density of $\rho = 2.30$ g/cm^3. The soft coating had $c_L = 1250$ m.s^{-1} and $\rho = 1.12$ g/cm^3.

E. Reference Models and Thickness Estimation

Theoretical predictions were provided by elastic guided-wave modes for a liquid-coated (LC) empty tube.[11] The fundamental flexural mode of the first circumferential order, $F_{LC}(1,1)$, was used to predict the outcome of the FFGW experiments. Wall thickness was estimated by fitting FFGW experiments by this model,[11] in which wall thickness can be computed as functions of phase or group velocities. The geometric and material parameters were the same than those listed in Sec. II D.

III. RESULTS

Figure 2 shows the distance-time diagrams recorded for a classical and decoded BSGC excitation with $2^n = 16$ (n = 4) times temporal averaging in a 3 mm tube, without and with a high-voltage amplification. Figure 3 illustrates the SNR of the FFGW as a function of averaging ($2^n = 4$-128, n = 2-7).

The SNR improvement obtained by averaging was 2.8 ± 0.3 dB/2^n, which resulted in -6.5 ± 0.5 dB SNR (at $2^n = 16$). Even after low-pass filtering the FFGW wave packet remained noisy (Fig. 2(a)). It was impossible to extract FFGW in the case of unamplified classical excitation (Fig. 2(b)). An amplified BSGC excitation generated a FFGW wave packet (Fig. 2(c)) with a 20 ± 1 dB SNR ($2^N = 16$). In this case SNR did not significantly improve with averaging, instead it asymptotically approached a 21 dB level (Fig. 3). An unamplified BSGC excitation generated a FFGW wave packet (Fig. 2(d)) with a 13 ± 2 dB SNR ($2^n = 16$) and a 2.5 ± 1.0 dB/2^N slope (Fig. 3). The unamplified and amplified BSGC excitation and the classical excitation provided qualitatively similar wave packets.

For the five tube samples (wall thickness 1-5 mm) the phase velocity, determined by 2D-FFT, remained consistent with that theoretically predicted by the $F_{LC}(1,1)$ mode, and fitting the measured FFGW velocity by the $F_{LC}(1,1)$ prediction yielded a proper thickness estimate, featuring a (0.41 ± 0.23)-mm $(14 \pm 6$ %; at 27 kHz) RMS deviation from the true wall thickness (Fig. 4). At 25 and 30 kHz we detected an FFGW consistent with the $F_{LC}(1,1)$ mode in some, but not all samples. At 27 kHz we found $F_{LC}(1,1)$-like results for all samples.

IV. DISCUSSION

The SNR saturated at 21 dB (Fig. 3) as theoretically predicted by Eq. (1). The reconstructed BSGC response included artifacts from the convolution and white noise. SNR was defined as the ratio of the intensity of the signal and that of either artifact or noise, whichever was higher.

To reach 21-dB SNR by temporal averaging would require further amplification by +39 dB (starting from -18 dB level at N = 1 as seen for classical excitation with 80 V drive in Fig. 3), which is equivalent to N = 2^{13} = 8192 times the temporal averaging. Hence the BSGC excitation speeded up the measurement by at least a factor of $(1/2) * 2^{13}/2^5 = 2^8/2 = 128$. This accounts for the fact that BSGC excitation reached a 21-dB SNR effectively at N=2^5, and that the repetition
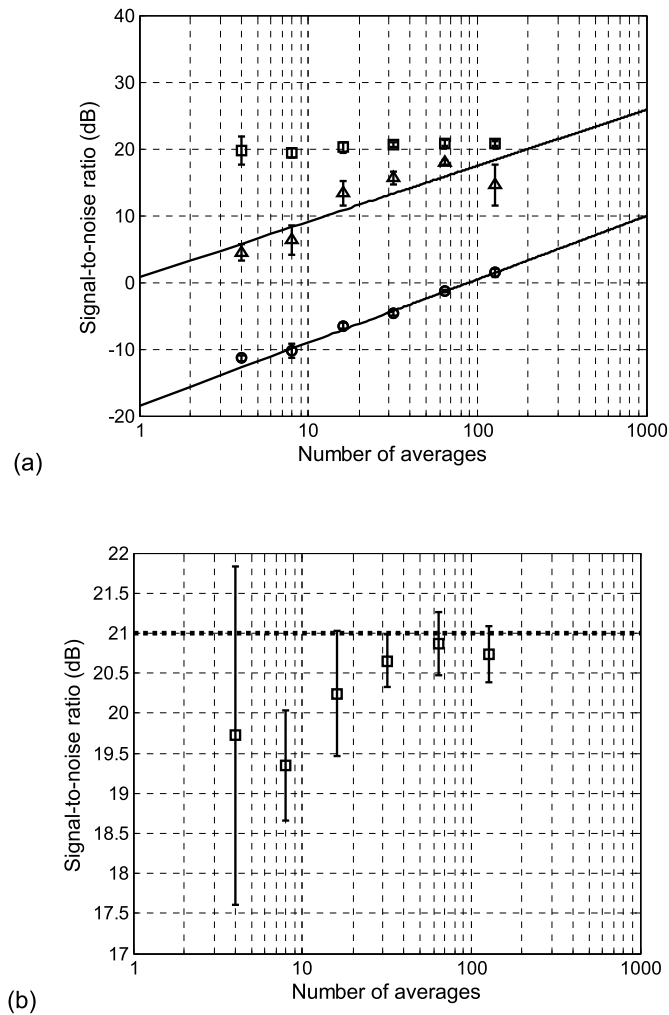
FIG. 3. (a) SNR of the received FFGW as a function of averaging, excited by a 80-V classical 4-cycle tone burst (circles), by a 10-V BSGC (triangles), and by an 80-V BSGC (squares). Solid lines visualize the slopes of the increase in SNR with increasing averaging, determined by the method of least mean squares. (b) A magnified view visualizes the approach to the 21-dB limit (dashed line). Error bars show the reproducibility in triplicate experiments. Results are shown for a 27-kHz excitation in a 3-mm tube with a 5-mm coating.

interval of BSGC excitation was two times longer (accounting for the emission time of the code pair) than that of the classical excitation. In particular, 21-dB SNR gain could be obtained at $N = 2^{21/2.8} = 180$ by classical excitation, given the 2.8 ± 0.3 dB/2^n slope of SNR gain observed, or almost a hundred times faster at $N = 2^1$ (a code pair) by BSGC excitation. For instance, our results suggest that a 10-dB SNR with an amplified classical excitation requires 2^{10} times averaging, which would take 3.5 min to perform with 40 source-receiver distances and a 200-Hz pulse-repetition rate. The corresponding result could, with BGSG, be obtained in two seconds provided that the mechanical translation were swift. Although this is merely an example and the speed up depends on the specific setup and amplification, a few seconds in contrast with minutes makes a difference in the applicability of the proposed technique e.g. for *in vivo* bone measurements.

   To some extent one may also gain in SNR by adding power amplification. For equivalent performance with our BSGC results, an additional 39 dB amplification is needed, which would imply going from a 80-V drive amplitude to a 7-kV drive.

   Importantly, we showed that despite the significant reduction in the measurement duration, the ability of an FFGW-based wall thickness assessment was maintained (Fig. 4). Related er-ror bars (0.41 ± 0.23 mm; 14 ± 6 %; at 27 kHz) were similar to or slightly higher than those
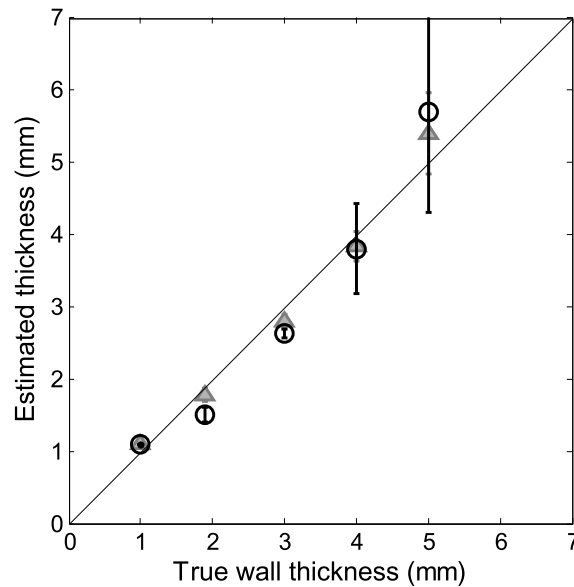
FIG. 4. Ultrasonic thickness estimate (at 27 kHz; circles) with respect to the true wall thickness. Related results from Ref. 7 (gray markers) are shown for comparison. Error bars show the reproducibility in triplicate experiments. Identity of the estimated and true thicknesses is represented by the solid line.

(0.23 ± 0.12 mm; 8 ± 3 %) recently obtained for an uncoded (photo-acoustic) excitation.[11] The difference between these results is explained by the different implementations of the excitation setup and differences in the signal analysis.

Given that poor SNR is an issue for non-contact methods, our results suggest that a coded excitation improves SNR in such situations, where signal cannot be distinguished from (white) noise at the receiver. In particular, it was shown that a coded excitation enhanced the displacement sensitivity of the optical US reception. This enhancement allowed the FFGW detection through a soft-tissue-mimicking coating, using a low source power. Our results thus suggest that a BSGC excitation could permit a non-contact measurement of FFGW *in vivo*.

Yet, our results suggest that a coded excitation may also facilitate using contact ultrasound transducers for FFGW excitation. A small foot-print 220-kHz piezo ($\varnothing = 10$ mm) was driven at 25-30 kHz. This was possible since the driving waveforms featured narrow bands (30-48% i.e. 8-13 kHz at the 27 kHz center frequency) so as to pass the piezo transducer without being critically distorted. The reduced transmitting efficiency (20-25 dB reduction in SNR) was compensated by using a BSGC excitation. Such low ultrasound frequencies improve the ratio of the acoustic power of FFGW to that of disturbing waveforms received on top of a soft coating.[11] Standard piezo elements at a frequency range of tens of kHz would be too large for the present purpose.

It was observed that the experimentally excited FFGW was not always consistent with the $F_{LC}(1,1)$ mode. In these cases it was represented or influenced by other (disturbing) modes such as $L_{LC}(0,1)$ or $L_{LC}(2,1)$, also present in the same frequency range. The selectivity of FFGW excitation can be improved e.g. by phased excitation.[12,13]

In this work, we evaluated the suitability of using BSGC excitation with a piezo transmitter. However, since photo-acoustic excitation of FFGW has advantages compared to piezo, in the future it will be relevant to continue research and focus on implementing a coded photo-acoustic transmitter[24,25] for wall thickness assessment.

V. CONCLUSION

A BSGC excitation speeded the pick up of FFGW in coated tubular phantoms by a factor of 100, while maintaining the capacity to be sensitive to wall thickness (thickness of the solid

wall was determined with a 14 ± 6 % precision). This makes the technique viable for time-critical measurements, such as samples that are moving, change as a function of time or measurement of *in vivo* samples.

ACKNOWLEDGMENTS

[1] P. Nagy and L. Adler, Journal of Applied Physics **66**(10), 4658-4663 (1989).

[2] I. A. Viktorov, *Rayleigh and Lamb waves: Physical theory and applications* (1967).

[3] J. L. Rose, Transactions-American Society of Mechanical Engineers Journal of Pressure Vessel Technology **124**(3), 273-282 (2002).

[4] Z. Su, L. Ye, and Y. Lu, Journal of sound and vibration **295**(3), 753-780 (2006).

[5] J. Foiret, J. G. Minonzio, C. Chappard, M. Talmant, and P. Laugier, Ultrasonics, Ferroelectrics, and Frequency Control, IEEE Transactions on **61**(9), 1478-1488 (2014).

[6] P. Moilanen, M. Talment, P. H. F. Nicholson, S. Cheng, J. Timonen, and P. Laugier, Journal of the Acoustical Society of America **122**(3), 2439-2445 (2007).

[7] J. N. Barshinger and J. L. Rose, Ultrasonics, Ferroelectrics, and Frequency Control, IEEE Transactions on **51**(11), 1547–1556 (2004).

[8] W. Luo and J. L. Rose, Journal of the Acoustical Society of America **121**(4), 1945–1955 (2007).

[9] R. Kirby, Z. Zlatev, and P. Mudge, Journal of Sound and Vibration **332**, 5040–5058 (2013).

[10] B. Yu, S. Yang, C. Gan, and H. Lei, Journal of Nondestructive Evaluation **32**(3), 263-276 (2013).

[11] P. Moilanen, M. Talmant, V. Kilappa, P. Nicholson, S. L. Cheng, J. Timonen, and P. Laugier, Journal of the Acoustical Society of America **124**(4), 2364-2373 (2008).

[12] P. Moilanen, Z. Zhao, P. Karppinen, T. Karppinen, V. Kilappa, J. Pirhonen, R. Myllylä, E. Hæggström, and J. Timonen, Ultrasound Medicine and biology **40**(3), 521-531 (2014).

[13] P. Karppinen, A. Salmi, P. Moilanen, Z. Zhao, R. Myllylä, J. Timonen, and E. Hæggström, Journal of Applied Physics **113**, 144904 (2013).

[14] C. E. Cook and W. M. Siebert, IEEE Transactions on Aerospace and Electronic Systems **24**(6), 825-833 (1988).

[15] M. Garcia-Rodriguez, Y. Yanez, M. J. Garcia-Hernandez, J. Salazar, A. Turo, and J. A. Chavez, NDT & E International **43**(8), 677-686 (2010).

[16] Q. Peng and L. Zhang, Ultrasonics, Ferroelectrics, and Frequency Control, IEEE Transactions on **58**(1), 122-133 (2011).

[17] X. Song, D. Ta, and W. Wang, Ultrasonics, Ferroelectrics, and Frequency Control, IEEE Transactions on **59**(11), 2580-2583 (2012).

[18] M. Golay, Complementary series. IRE Transactions on Information Theory **7**(2), 82-87 (1961).

[19] R. Chiao and X. Hao, Ultrasonics, Ferroelectrics, and Frequency Control, IEEE Transactions on **52**(2), 160-170 (2005).

[20] P. Laugier, Ultrasonics, Ferroelectrics, and Frequency Control, IEEE Transactions on **55**(6), 1179-1196 (2008).

[21] I. Nunez, R. Ing, C. Negreira, and M. Fink, Journal of the Acoustical Society of America **107**(5), 2370–2378 (2000).

[22] D. Alleyne and P. Cawley, Journal of the Acoustical Society of America **89**(3), 1159-1168 (1991).

[23] P. Moilanen, P. H. F. Nicholson, V. Kilappa, S. Cheng, and J. Timonen, Ultrasound in Medicine andBiology **32**(5), 709-719 (2006).

[24] M. Mienkina, C.-S. Friedrich, N. Gerhardt, W. Wilkening, M. Hofmann, and G. Schmitz, Ultrasonics, Ferroelectrics, and Frequency Control, IEEE Transactions on **57**(7), 1583–1593 (2010).

[25] S.-Y. Su and P.-C. Li, Optics Express **19**(2), 1174–1182 (2011).